A study of adsorption of cadmium, copper and lead by two clays from Burkina Faso

Brahima SORGHO [1*], Boubié GUEL [2], Lamine ZERBO [1], Moussa GOMINA [3]
et Philippe BLANCHART [4]

[1] *Materials Physical, Chemistry and Technology Team, Department of Chemistry, University of Ouagadougou, Burkina Faso.*
[2] *Physical Chemistry and Electrochemistry Team, Department of Chemistry, University of Ouagadougou, Burkina Faso.*
[3] *Ecole Nationale Supérieure d'Ingénieurs de Caen (ENSICAEN), Laboratoire de Cristallographie et Sciences des Matériaux (CRISMAT), Caen, France.*
[4] *Ecole Nationale Supérieure de Céramique Industrielle (ENSCI), Institute of Research for Ceramics –IRCER, Limoges, France.*
[*] *Corresponding author; E-mail: sorghobrahima3@gmail.com; 03 BP 7021 Ouagadougou 03 Burkina Faso.*

ABSTRACT

Water pollution caused by natural and anthropogenic causes become a major problem for many countries around the world in trying to find adequate and accessible means of treating polluted water. For more than a decade, research is focused on local adsorbent materials such as clays. It is in this dynamic that two clays extracted in Burkina Faso and referenced KORO and SIT were used to evaluate their capacities to reduce the content of heavy metals in aqueous solutions simulating waste water. The monitoring of the removal processes uses electrochemical characterizations, as voltammetry, evidencing a removal degree of heavy metals exceeding 90%. Characterizations of the process were also obtained by X-ray diffraction, Infrared Spectroscopy and Scanning Electron Microscopy. It is shown that the removal process occurs through the formation of clay-heavy metals complexes with both KORO and SIT. The three major mechanisms that were evidenced are complexation, ion-exchange and precipitation.
© 2018 International Formulae Group. All rights reserved

Keywords: Clay; adsorption; heavy metals; waste water; removal.

INTRODUCTION

Water resources (surface water and groundwater) in many of the Sahelian countries face pollution due to population growth and industrial development (Nlend, 2018; UNIDO, 2013; Okorie, 2014; Gouin, 2016; Tamungang, 2016; Baby, 2010). The pollutants encountered in water are mostly heavy metals produced by anthropogenic activities as industrial wastes, agricultural

chemicals, etc. In general, they are highly toxic with dangerous impacts on human, animal and plant health (Rudnai et al., 2014; Marsden and Philip, 2003). Besides, the population growth now creates a great need of pure water resources, avoiding toxic elements as heavy metals. Consequently, some researches from the scientific community contribute in finding adequate and accessible water treatment techniques, and some of them are based on surface properties of phyllosilicates minerals in contact to aqueous solutions. The use of clays in purification of contaminated water by heavy metals necessitate a deep knowledge of their mineralogical, physical and chemical characteristics in relation with their surface chemistry in contact with waste water.

In Burkina Faso, only few studies (Traore et al., 2000; Potgieter et al., 2006; Keita, 2014; Ghorbel-Abid, 2015; Sorgho et al., 2016) were devoted to clays used as adsorbents for the removal of heavy metals, although they have been the subject of several studies at the international level. At present, new researches in African laboratories are a preliminary response to the imperative needs for water treatment. Objectives are within the most recent Sustainable Development Objectives of United Nations, for a large access of peoples to pure water and for the management of sustainable water resources. In this work, two clays mined in Burkina Faso, named KORO and SIT are used for studying the removal of Cd^{2+}, Cu^{2+} and Pb^{2+} in contaminated waste water.

MATERIALS AND METHODS
Materials

The KORO and SIT clays were taken from different local clay sites. Table 1 summarizes the characteristics of the clay samples, the sampling sites and the geographic coordinates. The locations of the

sites are indicated on the map of Burkina Faso (Figure 1). Both clays, KORO and SIT have already been characterized in earlier work (Kam et al., 2009; Sorgho et al., 2016).

Experimental methods
Characterization of raw materials

The mineralogical phases were identified by X-ray diffraction (XRD) on powders with a Brüker D8 Advance diffractometer, with CuKα source and equipped with a graphite back monochromator, operating at a voltage of 40 kV and intensity of 50 mA.

Chemical analyses of clays were performed by ICP-OES (Inductively Coupled Plasma Optical Emission Spectroscopy), with a Perkin Elmer Optima 7300V HF. Microwaves assisted dissolution were obtained in both hydrochloric acid (HCl) and nitric acid (HNO_3).

The cation exchange capacity (CEC) and the specific surface area (SSA) were determined using the methylene blue isotherm method as described in the literature (Savic, 2014; Karimi, 2011; Sorgho et al., 2016). A method using the ethylene diamine of copper (Bergaya and Vayer, 1997) was also used to correlate the CEC values since the thermodynamic values relative to the formation of complexes are known. This method was successfully used with different clays to characterize ion exchange with heavy metals in a large range of pH.

The morphologies of clay powders were characterized by SEM with a HITACHI SC-2500 apparatus.

The acid-base assays were carried out using a similar method than that described in previous publications (Sajidu et al., 2006; Sorgho et al., 2016). For pH measurements, we used a combined pH electrode from Ross Sure Flow Orion (No. 8172) connected to a PH-meter Orion 940. The acid-base titration

curves were used to determine the pH at point of zero charge (Sajidu et al., 2006; Sorgho et al., 2016).

Preparation of Cd²⁺, Cu²⁺ and Pb²⁺ solutions

To prepare representative clay dispersions, 1 g of each clay was mixed with 100 mL of NaNO₃ solution with a concentration of 1 mol/L. Mixtures were stirred during 1 hour before being centrifuged for 15 min at 3000 rpm. After pouring the supernatant, settled clays were washed with a NaNO₃ solution, with a concentration 0.05 mol/L. Clays were added to 100 mL of NaNO₃ (0.05 mol/L) and stirred during 24 hours for the hydration of mineral phases. Model solutions of metal were prepared with pure salts of Cd(NO₃)₂.2H₂O, CuCl₂.2H₂O and Pb(NO₃)₂. Obtained concentrations were 20 μmol/L of Cadmium, 35.4 μmol/L of Copper and 10.86 μmol/L of Lead.

Adsorption processes were characterized with 10 mL of each clay dispersion mixed with 10 mL of each metal solution. Along the process, pH was maintained between 2 and 12 and mixtures were stirred during 48 hours. Afterwards, they were centrifuged, and pH of supernatants were controlled. Residual concentrations of metals were measured by an electrochemical method.

Concentrations in solutions of Cd²⁺, Cu²⁺ and Pb²⁺

Concentrations were measured by anodic stripping voltammetry that is a voltammetry method for the quantitative determination of many ionic species and most particularly heavy metals. During the deposition step at the beginning of the analyze, an analyte was obtained by electroplating on a working electrode. After precisely 2 min, electrolysis and stirring are ended and the stripping step begins. It is an oxidation step involving the measurement of the electrode current. During oxidation, registered current attains peak values that correspond to the potential at which the species begin to oxidize. In this study, we used a method with differential pulses of current for the accurate determination of Cd²⁺, Cu²⁺ and Pb²⁺.

For experiments, we used a potentiometer (PST050 Radiometer Analytical), a polarographic stand (MDE150 Radiometer Analytical), a measuring cell with a rotating disc electrode, a silver chloride reference electrode Ag/AgCl (3M KCl), an auxiliary platinum electrode for measuring the current flowing through the indicator electrode, and a nitrogen inlet for the bubbling in the solution.

The removal efficiency of a metal in solutions R (%) was determined by Eq. (1):

$$R(\%) = \left(1 - \frac{c}{c_0}\right).100$$

(Eq. 1)

Where: C_0 and C are the initial and final concentrations respectively of the metal ions in solution.

Table 1: Geographical coordinates of clay sites for the two clays of Burkina Faso.

Reference	Area of mining	Geographical coordinates	
		Latitude North	Longitude West
KORO	Koro site;15 km from Bobo-Dioulasso city	11,15°	04,18°
SIT	Sitiéna; 10 km from Banfora city	10,36°	04,48°

Figure 1: Geographical areas of clay mining sites.

RESULTS

Based on characterization of KORO and SIT clays that were already published (Kam et al., 2009; Sorgho et al., 2016), the mineralogical compositions of the two mineral materials are reported in Table 2. It evidences that KORO and SIT clays have similar mineralogical compositions excepted for the higher goethite content in KORO clay. The values of CEC and Specific Surface Area (SSA) obtained by the methylene blue method and the ethylene diamine copper method are also summarized in Table 2. CEC and SSA values are in between values reported in the literature for many smectites clays (CEC = 80-150 meq/100 g and SSA = 700-800 $m^2 \cdot g^{-1}$) and for kaolinite clays (CEC = 5-15 meq/100g and SSA = 10-30 $m^2 \cdot g^{-1}$) (Sorgho et al., 2016).

Figure 2 and Figure 3 present the acid-base titration curves of KORO and SIT (Figure 2 and Figure 3), we obtained equilibrium pH in pure water of 7.23 (KORO) and 6.54 (SIT). They show that the equilibrium pH in pure water are different for the two clays. The interpretation of acid titration curves leads to the determination of the necessary acid content V_e for attaining the equilibrium volume (Sajidu et al., 2006). Values of pH_{PCN}= 7.31 for KORO and pH_{PCN}= 6.66 for SIT were calculated from the $pK_{a1, app}$ and $pK_{a2, app}$ as indicated in acidity constant curves of Figure 4 and Figure 5.

In Figures 6, 7 and 8, the adsorption curves of heavy metals against the equilibrium pH, were obtained by anodic stripping voltammetry. It evidences a significant removal efficiency of Cd^{2+}, Cu^{2+} and Pb^{2+} ions in a large pH range, from pH 2 to 12.

In Figure 6, the adsorption curves of Cd^{2+} against the equilibrium pH evidence variations in the removal efficiency. For SIT, at pH = 2.63, the efficiency is 19.70% and for KORO the efficiency decreases to 0.47%. For pH = 9.7, the removal efficiency increases up to 91% for SIT and 89% for KORO.

The Figure 7 shows that Cu^{2+} is removed from solutions at pH of 2.60 with an efficiency of 35.94% for SIT and 42.98% for KORO. The efficiency increases to attain 97.30% for SIT and 96.59% for KORO just below pH = 6.55.

In Figure 8 for pH= 5.50, we observe that lead is removed with a high efficiency of 99% for the two clays. At pH= 2.66, the removal efficiency is 71.79% for KORO and at pH= 2.60, it attains 96.12% for SIT. The removal process attains a plateau value above pH= 5.50, evidencing an efficiency of 99.87%.

Figure 9 presents X-ray patterns of KORO after reaction processes in solutions. In similar experimental conditions, Figure 10 presents the X-ray pattern of SIT clay. For KORO, the X-ray patterns (Figure 9) after the reaction processes in solutions show variations in many reflection intensities and

profile that suggest the interaction of most of minerals in the removal processes of heavy metals. For SIT (Figure 10), the significant peak of montmorillonite changes, but also for other minerals evidence the occurrence of strong interactions between species in solution and the clay.

IR spectroscopy are represented in Figure 11 for KORO clay and in Figure 12 for SIT clay. Figure 11 shows several changes in the infrared spectra that are similar to that already highlighted by some authors (Madejova et al., 1999; Madejova et al., 2006; Eren et al., 2008). In general, they attempted to clarify causes of band changes, but Eren et al., 2008 have explained that adsorption of Cu(II) influences Si-O and OH bands from montmorillonite. In Figure 12 for SIT clay after adsorption, we observe that heavy metals (Cd^{2+}, Cu^{2+} and Pb^{2+}) change the nature of SIT surfaces. However, changes are similar to that of KORO and are also described in works of some authors (Madejova et al., 1999;

Madejova et al., 2006; Eren et al., 2008; Eren et al., 2009; Fonseca et al., 2009; Shütz, 2016). As for KORO clay, they are helpful for the recognition of interaction mechanisms between heavy metals and clay minerals.

Microstructural observations by SEM are in images of KORO and SIT in Figure 13 and Figure 14 respectively. All figure present both aspect of microstructures and the chemical composition by EDS that is averaged on the image surface. In Figure 13 and Figure 14, SEM images of KORO and SIT illustrate the typical morphology of phyllosilicates minerals. After reaction with heavy metals, morphologies have a more agglomerated appearance, which show the adsorption processes of heavy metals. The clay particle agglomeration in mixtures could be due to the trapping of the metal ions by the clay platelets. Besides, we observe small nodules on surface of clays that should results from the formation of metal complexes and precipitates.

Table 2: Mineralogical compositions of KORO and SIT clays.

Mineral	KORO (%)	SIT (%)
Albite (Si_3AlO_8Na)	12	16
Kaolinite ($Al_2Si_2O_5(OH)_4$)	7	19
Goethite ($FeO(OH)$)	7	-
Illite ($(K,H_3O)Al_2Si_3AlO_{10}(OH)_2$)	21	11
Montmorillonite ($(Al_{1,67}Mg_{0,33})Si_4O_{10}(OH)_2Na_{0,33}$)	26	26
Quartz (SiO_2)	15	13
Orthoclase ($KAlSi_3O_8$)	8	7
Balance	4	6

Table 3: Specific surface areas (SSA) and Cation Exchange Capacity of mined clays.

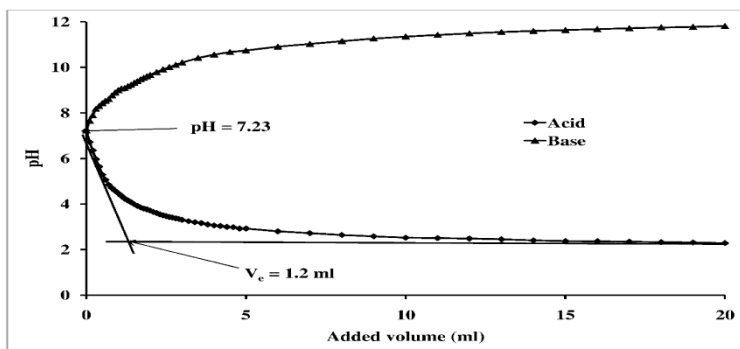| Samples	CEC (meq/100g of clay)		SSA ($m^2 \cdot g^{-1}$)
	Methylene blue method	Ethylene diamine of cooper	Methylene blue method
KORO	41,35	42,38	323,77
SIT	51,63	53,58	404,26

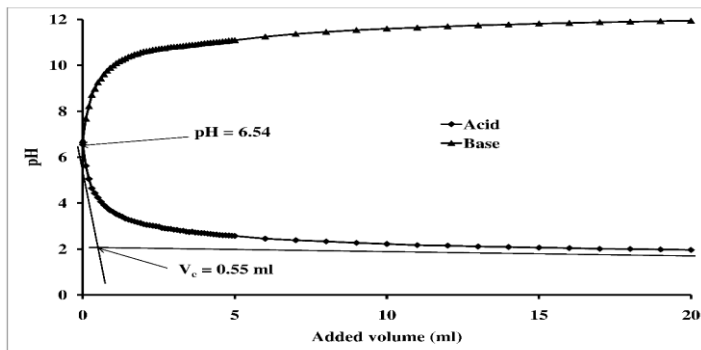**Figure 2**: Acid-base titration curves of KORO in water.

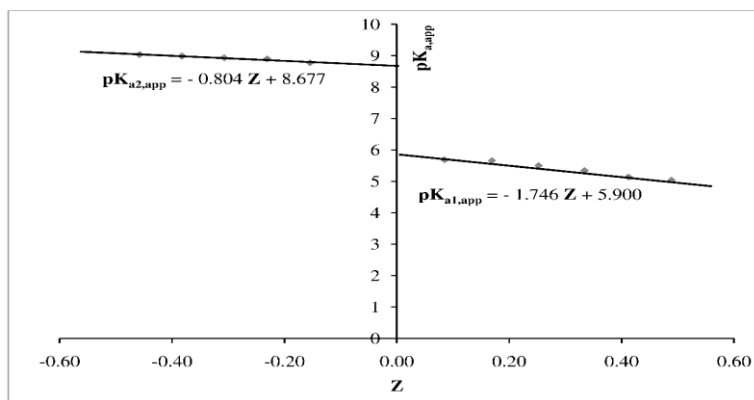**Figure 3:** Acid-base titration curves of SIT in water.

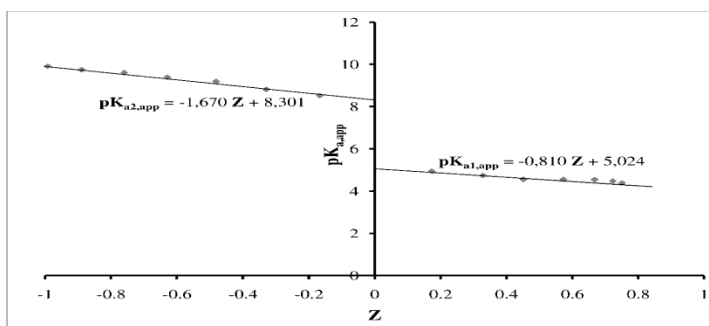**Figure 4**: Acidity constants ($pK_{a,app}$) against electrostatic charge Z for KORO.

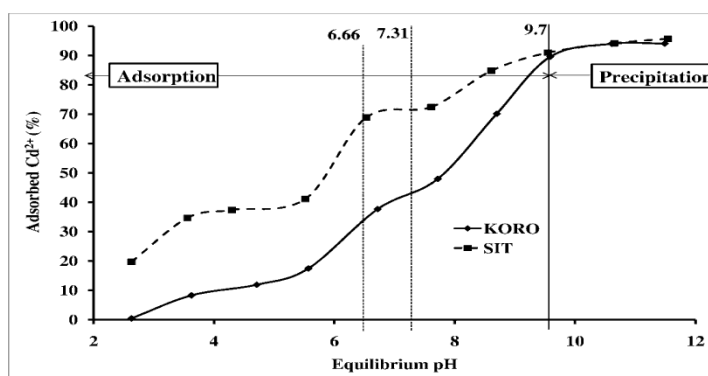**Figure 5**: Acidity constants ($pK_{a,app}$) against electrostatic charge Z for SIT.

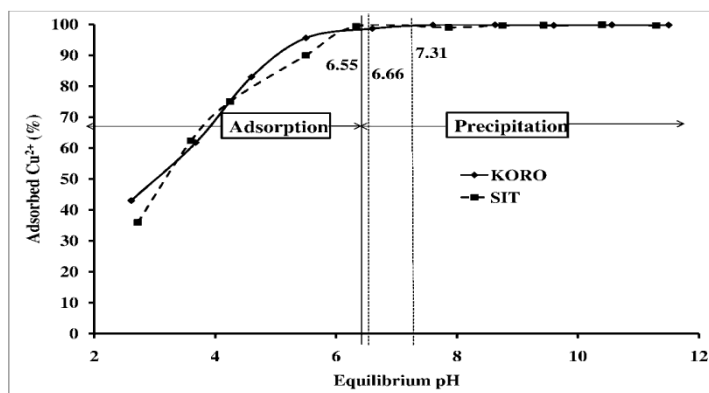**Figure 6**: Adsorption curves of Cd^{2+} as a function of equilibrium pH.

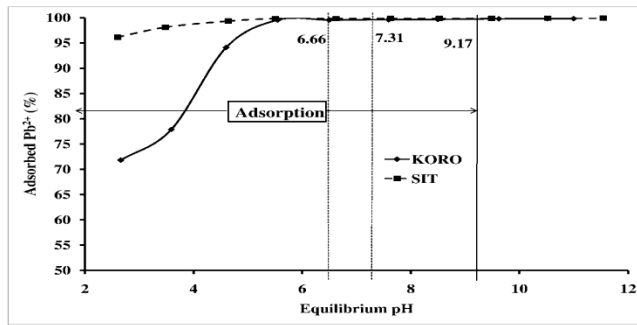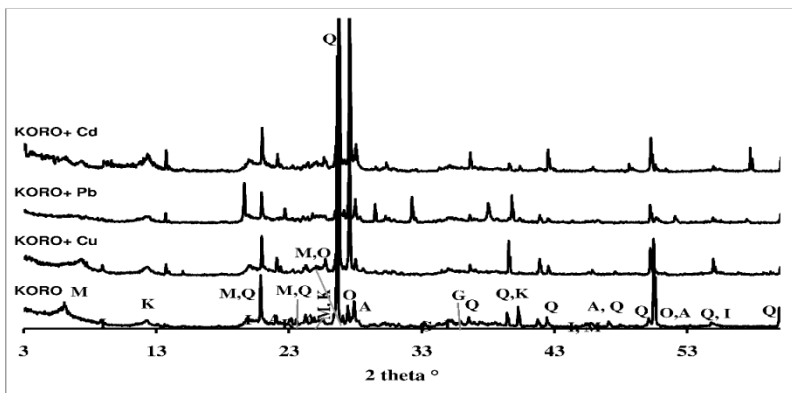**Figure 7**: Adsorption curves of Cu^{2+} as a function of equilibrium pH.

Figure 8: Adsorption curves of Pb^{2+} as a function of equilibrium pH.

Figure 9: Diffraction patterns of KORO, KORO-Cd^{2+}, KORO-Cu^{2+} and KORO-Pb^{2+}.
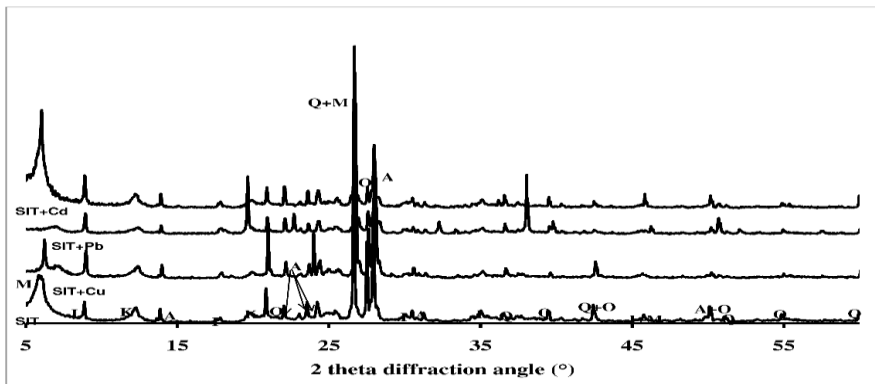
Figure 10: Diffraction patterns of SIT, SIT-Cd^{2+}, SIT-Cu^{2+} and SIT-Pb^{2+}.
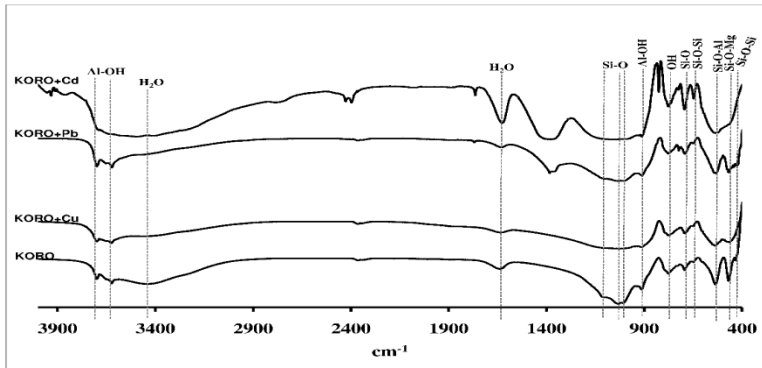
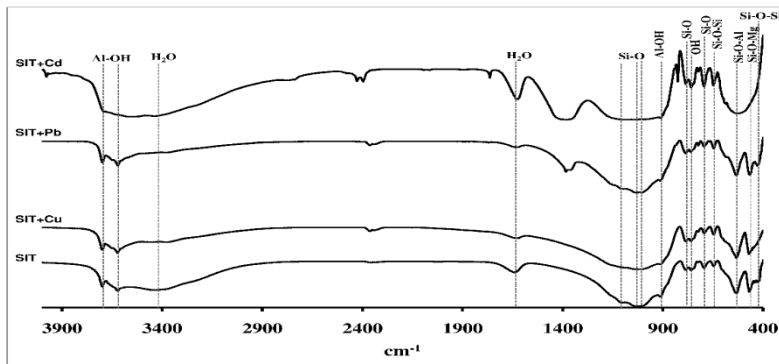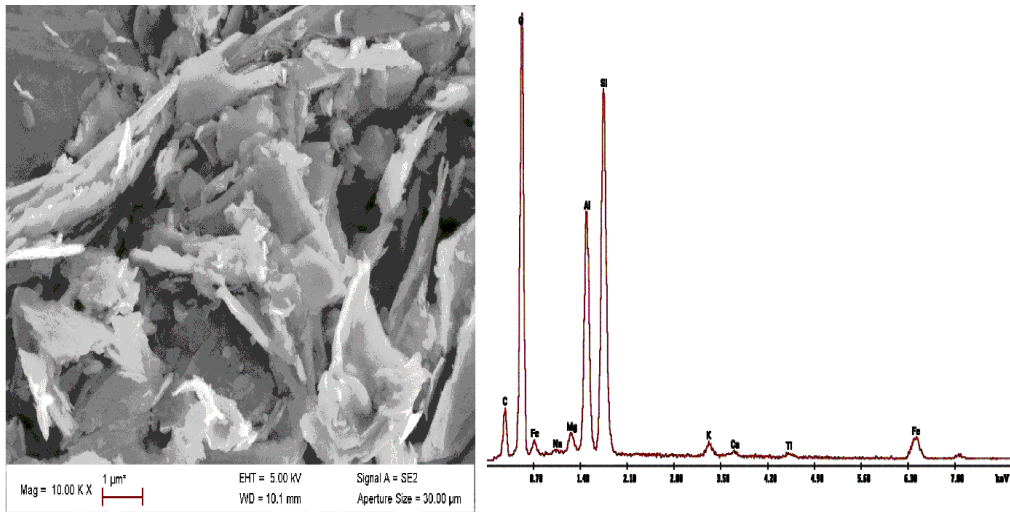**Figure 11:** Infra-Red spectra of KORO, KORO-Cd^{2+}, KORO-Cu^{2+} and KORO-Pb^{2+}.

Figure 12: Infra-Red spectra of SIT, SIT-Cd^{2+}, SIT-Cu^{2+} and SIT-Pb^{2+}.

A

B
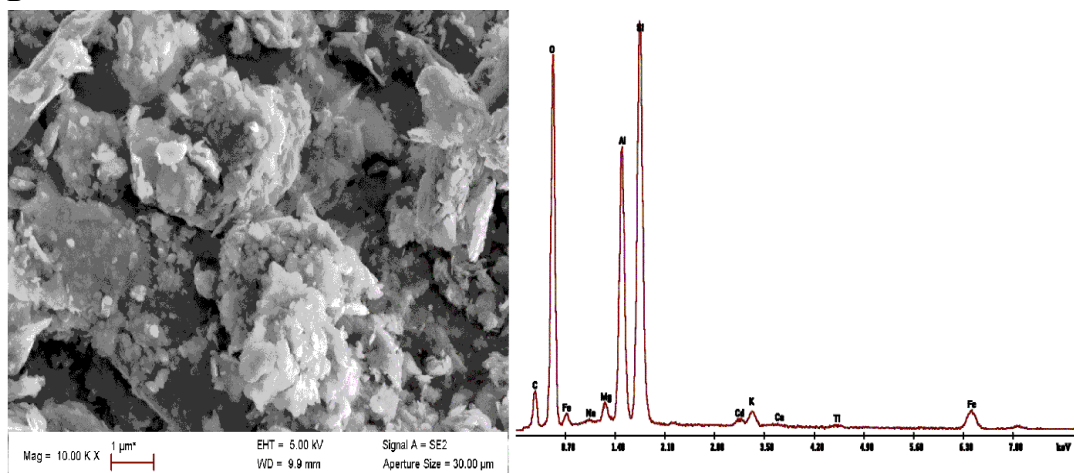
C
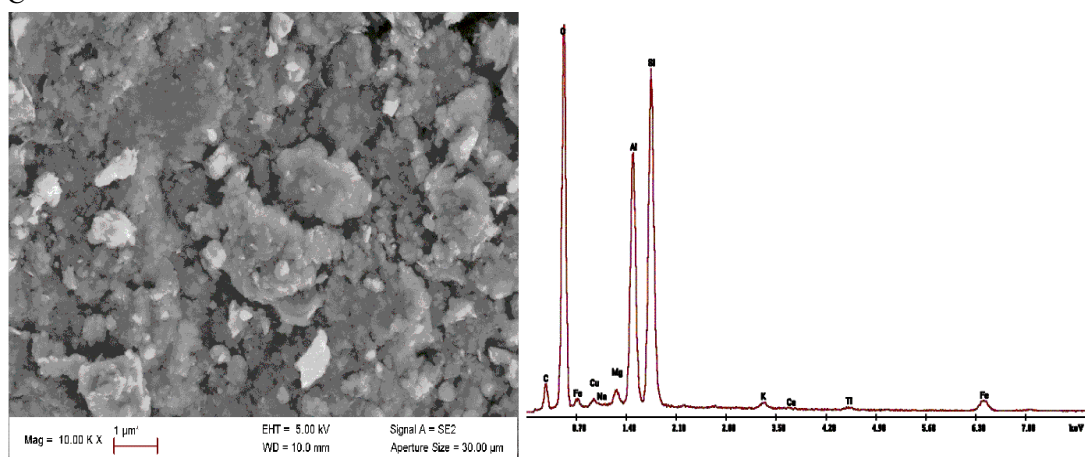
D
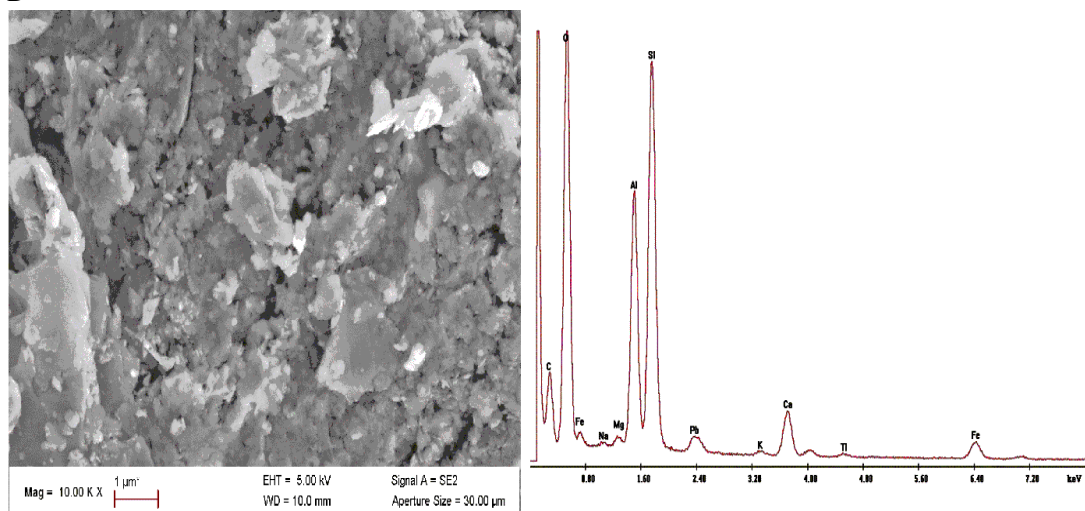
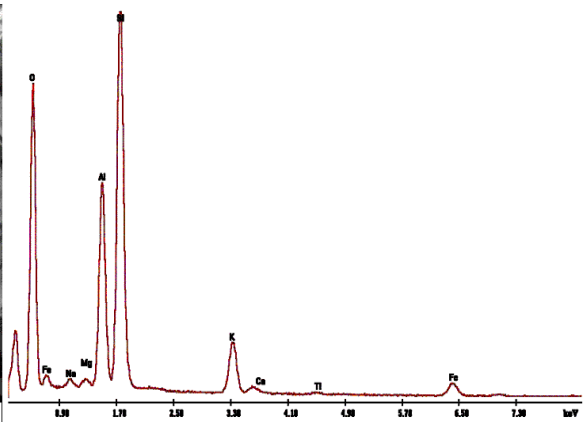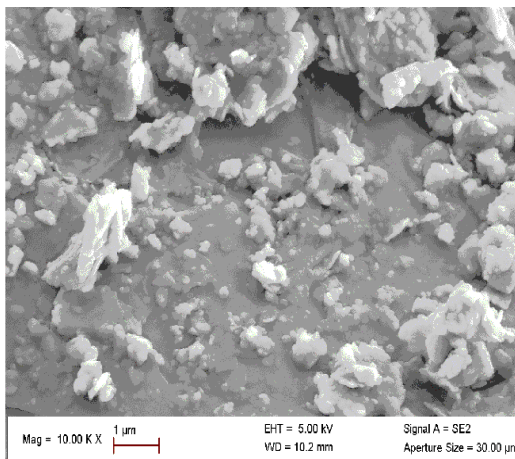**Figure 13:** SEM images and EDS analyses for(A) KORO, (B) KORO-Cd^{2+}, (C) KORO-Cu^{2+} and (D) KORO-Pb^{2+}.

A
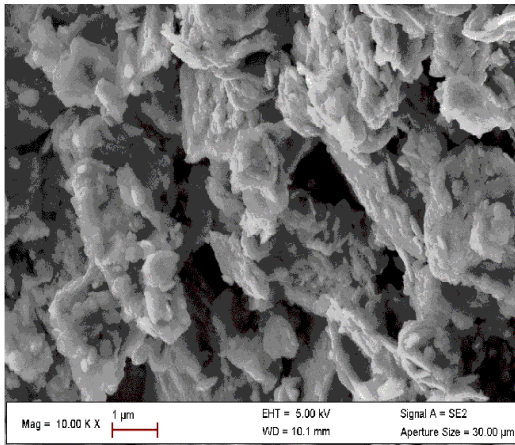
B
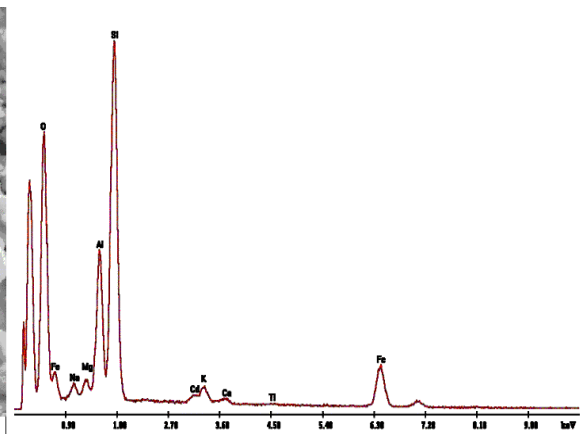
C

D
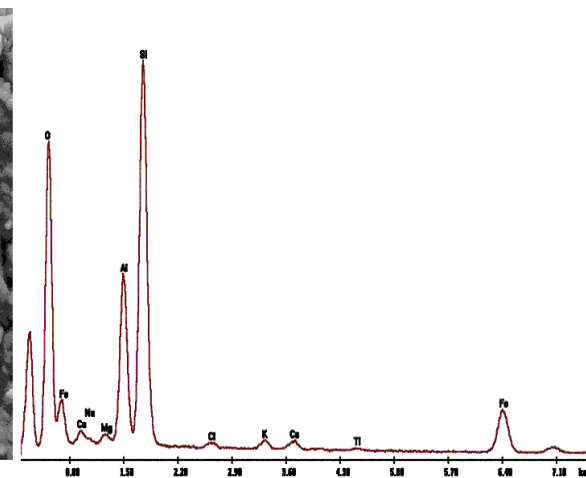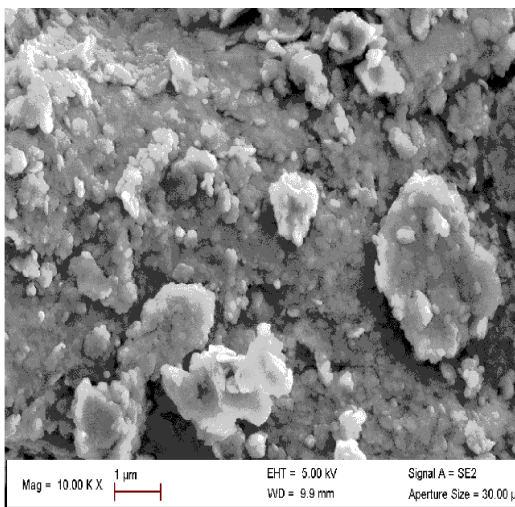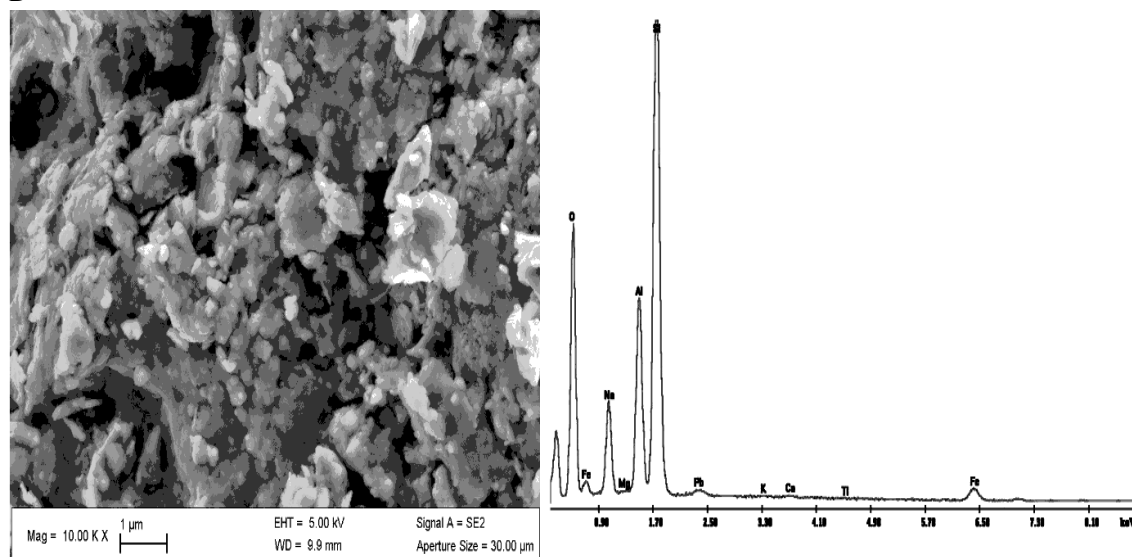
Figure 14: SEM images and EDS analyses for (A) SIT, (B) SIT-Cd^{2+}, (C) SIT-Cu^{2+} and (D) SIT-Pb^{2+}.

DISCUSSION
Characterization of raw materials

The mineralogical compositions of KORO and SIT clays (Table 2) are not very different excepted for the higher goethite content in KORO clay. This would explain why the values of CEC and SSA of the two clays are relatively close. The intermediate values of CEC and SSA result in the presence of several mineral phases (Table 2) in the two samples (Sorgho et al., 2016).

Acid-base titration of clay dispersions

From the acid-base titration curves of KORO and SIT (Figure 2 and Figure 3), we note that the pH values in pure water shows that KORO is weakly basic (pH = 7.23) and SIT, weakly acidic (pH = 6.54). The values of pH$_{PCN}$ of KORO (pH$_{PCN}$= 7.31) and SIT (pH$_{PCN}$= 6.66) are relatively same to their pH values in pure water and that confirms the nature of the two samples.

Removal of Cd^{2+}, Cu^{2+} and Pb^{2+}
Cd^{2+} ions removal from solutions

The value pH= 9.7 is close the values at which Cadmium hydroxide precipitates (Cd(OH)$_2$), when the concentration of Cd^{2+} is 10^{-6} mol/l. It is also consistent with the pH value for the precipitation of cadmium hydroxide in a cadmium-water system, as described by the Pourbaix diagram (Nila, 1996). Above pH= 9.7, precipitation becomes predominant in the removal of cadmium, and the removal efficiency attains 94.12% and 93.95% for SIT and KORO respectively.

Below pH= 9.7, Cd^{2+} ions are predominant in solutions, according to the Pourbaix diagram. Ion removal in clay-solutions for the two clays is mainly due to adsorption that results from the formation of complex species on clay surfaces, together with ion exchange, since the removal of Cd^{2+} begins below pH$_{PCN}$ (7.31 for KORO, 6.66 for SIT) (Sajidu et al., 2006, Schütz, 2016).

Beside the above-mentioned mechanisms, iron oxides and organic matter associated to clays would also participate in the removal of cadmium metal from the solutions (Bradl, 2004).

Removal of Cu^{2+} ions

Considering the Pourbaix diagram (Nila, 1996) for the copper-water system, pH for precipitation is also close to 6.55. Below pH= 6.55 and although no precipitation occurs, more than 90% of Cu^{2+} is removed by both complexation on clay surfaces and ion exchange. It is supported by the adsorption process that begins before pH_{PCN} (7.31 for KORO, 6.66 for SIT) (Sajidu et al., 2006). Above pH= 6.55, the formation of precipitated copper species contributes to the removal of Cu^{2+}, and precipitation occurs for both KORO and SIT clays. The removal efficiency of copper attains 99.85% for SIT and 99.78% for KORO. For SIT and KORO, in addition to complexation and ion exchange, there would be different processes of complex formation from iron species and organic matter (Bradl, 2004).

Removal of Pb^{2+}

The maximum elimination rate is reached at pH= 5.50 before the pH= 9.17 which is the pH of formation of the lead hydroxide precipitates according to the Pourbaix diagram for the water-lead system. These results demonstrate that the predominant processes of lead removal would be complexation reactions on clay surfaces and ion exchange (Sajidu et al., 2006).

Structural Investigations

X-ray Diffraction of KORO clay

X-ray patterns of KORO (Figure 9) evidence differences in reflection intensities. Particularly, [130] and [011] reflections of

goethite at 33.25 2θ° and 35.71 2θ° respectively, are vanished in mixtures patterns. It would be related to the formation of goethite-heavy metals complexes.

On the pattern of KORO-Cd^{2+}, we observe the splitting of the [001] reflection of montmorillonite that is initially at 6.06 2θ°. The reflection situated in initial position is related to unreacted montmorillonite with Cd^{2+} ions. A new reflection at 7.20 2θ°, would be from montmorillonite that have reacted in solution. The displacement of [001] reflection is due to an ion exchange phenomenon, when heavy metals are substituted in cationic sites (K^+, Na^+, Ca^{2+} ...) at montmorillonite interlayers. It changes interlayer spacing since metal cations (Cd^{2+}, Cu^{2+} and Pb^{2+}) have ionic atomic radii lower than that of substituted cations. Besides, the type of heavy metals also changes the nature of cation-water complexes in interlayers.

With bentonite-lead solutions, previous works have shown a similar displacement of the [001] reflection (Caglar et al., 2009; Chambi-Peralta, 2018; Monteiro., 2018). It was also evidenced with montmorillonite-copper solutions (Eren E. et al., 2008). Authors explained that the adsorption of copper induces structural changes in clay minerals.

In addition to the shift of reflection position, the decrease in intensity of the [001] reflection of montmorillonite in KORO-Pb^{2+} pattern would result from the formation of $Pb_3(CO_3)_2(OH)_2$ that precipitates in solution (Zhang et al., 2012). Variation of intensity of the [001] reflection of kaolinite at 12.11 2θ°, is related to the formation of complex species at silanol (-Si-OH) and aluminol (-Al-OH) sites, since kaolinite belongs to the TO mineral group with no cation exchanges at interlayers. The [002] reflection of illite at

8.82 2θ° increases in intensity in KORO-Cu^{2+} pattern but disappears in patterns from other mixtures. This change would be related to a reaction between clay minerals and heavy metals (Srivastava et al, 2005).

X-ray Diffraction of SIT clay

X-ray patterns of SIT below and after adsorption processes (Figure 10) evidence the significant variations of [001] reflection of montmorillonite at 5.85 2θ°. They are originated from similar phenomenon than that occurred with KORO mixtures. Particularly, changes in intensity of [001] kaolinite reflection, at 12.16 2θ°, are related to the formation of complex species at silanols (-Si-OH) and aluminols (-Al-OH) surface sites. With illite, the [002] reflection at 8.84 2θ° increases in intensity in the SIT-Cd^{2+}, SIT-Cu^{2+} and SIT-Pb^{2+}. Such increase in intensity is attributed to interaction between minerals and heavy metals. Beside phyllosilicate reactions, the [001] reflection of albite at 13.84 2θ° also decreases in intensity in SIT-Pb^{2+} pattern. It further supports an interaction between most of minerals in SIT and heavy metals.

Infrared spectroscopy

IR spectroscopy of KORO clay

In Figure 11, changes in band positions and profiles are mostly related to Si-O and OH bindings in montmorillonite. Besides, we observe the decrease of intensity of Si-O-Al bands from the same mineral at about 536 cm^{-1}. Fonseca et al., 2009 relates changes in typical clay mineral bands at 3699 cm^{-1}, 3622 cm^{-1} (Al-OH bands) and at 1030 cm^{-1} (Si-O) to their importance in the removal of metals. In the spectrum of KORO-Pb^{2+} and along with previous authors, we suggest that the variation of the OH band at 1645 cm^{-1} from adsorbed

water can be related to the formation of PbOH$^+$. In the low frequency region, changes in bands of Si-O-Al (536 cm^{-1}) and Si-O-Si (431 cm^{-1}) were also evidenced by Caglar et al., 2009 with montmorillonite. Further work of Eren et al., 2009 with bentonite-Pb (II) mixtures explains that Pb(II) ions induce Si-O bond changes in the region of 1200-950 cm^{-1}. New bands were also identified at 1764, 1384, 840, 826 and 730 cm^{-1} on the spectrum from KORO-Cd^{2+}. They must be related to reactions between clay and Cd^{2+} ions. With Pb^{2+}, new bands are identified at 1768, 1374, 840 and 726 cm^{-1} that are from reactions on surfaces of KORO minerals.
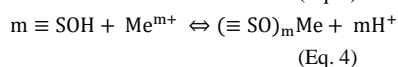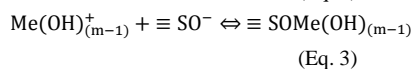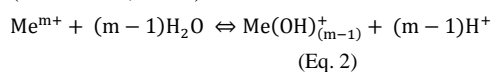
IR spectroscopy of SIT clay

IR spectra of Figure 12 for SIT further illustrate the adsorption process of Cd^{2+}, Cu^{2+} and Pb^{2+}. As for KORO, we observe changes of Si-O and OH bindings in montmorillonite and the decrease of intensity of Si-O-Al bands at 536 cm^{-1}. However, new bands at 1764, 846 and 826 cm^{-1} appear in the spectrum of SIT-Cd^{2+}. They are related to surface reactions with SIT. With Pb^{2+} ions, similar surface reactions are evidenced with new bands at 1768, 1380 and 844 cm^{-1}.

Microstructural investigations

Morphological changes in SEM images of KORO and SIT of Figure 13 and Figure 14 reveal the interaction of clays with solutions containing heavy metals. The chemical analyses by EDS of natural clays show that the content of heavy metals is low and below the detection threshold. After reactions in solutions, chemical analyses of white nodules and dark areas in clay surfaces reveal the presence of Cd^{2+}, Cu^{2+} and Pb^{2+}. This finding can be interpreted by an ion exchange process occurring in darker zones, and by

complexation and precipitation processes in nodules. Consequently, we suggest that heavy metals always react with clays, but adoption results from different mechanisms as complexation, ion exchanges and precipitation. The following mechanisms are proposed (Eq. 2 to 7):

In the case of a complexation mechanism (Eren et al., 2008):

$$Me^{m+} + (m-1)H_2O \Leftrightarrow Me(OH)^+_{(m-1)} + (m-1)H^+$$
$$(Eq. 2)$$

$$Me(OH)^+_{(m-1)} + \equiv SO^- \Leftrightarrow \equiv SOMe(OH)_{(m-1)}$$
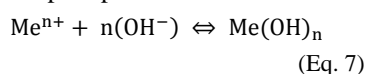$$(Eq. 3)$$

$$m \equiv SOH + Me^{m+} \Leftrightarrow (\equiv SO)_m Me + mH^+$$
$$(Eq. 4)$$

for ion exchange (Chen Chen et al., 2015; Barbier et al., 2000; Yavuz et al., 2003) :

$$nXC + Me^{n+} \Leftrightarrow X_n Me + nC^+$$
$$(Eq. 5)$$

$$mX_n C + nMe^{m+} + X_{n.m}Me_n + mC^{n+}$$
$$(Eq. 6)$$

for precipitation:

$$Me^{n+} + n(OH^-) \Leftrightarrow Me(OH)_n$$
$$(Eq. 7)$$
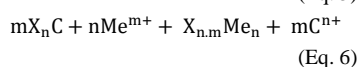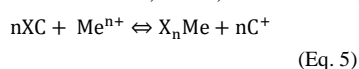
where $\equiv SO^-, \equiv S(OH)_2, \equiv SOH$ and X are on clay surfaces; S = Al, Si, Fe, Mn, Mg; Me are heavy metals; C and C^{n+} are interlayer cations (Na^+, Ca^{2+}, K^+…).

Conclusion

The used two clays from Burkina Faso (KORO and SIT) that have an equilibrium pH in pure water at pH=7.23 and 6.54, respectively. pH values are close to pH_{PZC} of both clays, which are 7.31 and 6.66 for KORO for SIT respectively. The use of clays for the removal of Cd^{2+}, Cu^{2+} and Pb^{2+} in a large range of pH proved the ability of the process since we obtain a removal ratio exceeding 90%. The monitoring of this elimination was made by voltammetry, which allowed measuring the concentrations of heavy metals as low as 10^{-9} L^{-1}. It would be due to a synergistic action of the different minerals contained in clays. Infrared spectroscopy, X-ray diffraction, scanning electron microscopy and EDS analyzes evidence that almost all minerals are involved in removal of the three heavy metals in solutions. It is achieved by three main mechanisms that are adsorption, trapping at clay platelets and precipitation. Microstructural investigations were helpful to evidence the occurrence of each mechanisms.

COMPETING INTERESTS

The authors declare that they have no competing interest about the work reported in this paper.

AUTHORS' CONTRIBUTIONS

Conception and design of the study: BS, BG, LZ, MG and PB. Data collection: BS, BG, LZ and PB. Draft of the article: BS and PB. Critical revision of the article for important intellectual content: BS, BG, LZ, MG and PB. All authors read and approved the final version of the manuscript.

REFERENCES

Baby J, Raj JS, Biby ET, Sankarganesh P, Jeevitha MV, Ajisha SU, Rajan SS. 2010. Toxic effect of heavy metals on aquatic environment. *Int. J. Biol. Chem. Sci.*, **4**(4): 939-952. DOI: http://dx.doi.org/10.4314/ijbcs.v4i4.62976

Barbier F, Duc G, Petit-Ramel M. 2000.

Adsorption of lead and cadmium ions from aqueous solution to the montmorillonite/water interface. *Colloids and Surfaces A: Physicochemical and Engineering Aspects,* **166**(1-3): 153-159. DOI: 10.1016/S0927-7757(99)00501-4

Bradl HB. 2004. Adsorption of heavy metal ions on soils and soils constituents. *J. Colloid Interface Sci,* **277**(1): 1-18. DOI: 10.1016/j.jcis.2004.04.005

Caglar B, Afsin B, Tabak A, Eren E. 2009. Characterization of the cation-exchanged bentonites by XRPD, ATR, DTA/TG analyses and BET measurement. *Chem. Eng. J.,* **149**(1-3): 242-248. DOI: 10.1016/j.cej.2008.10.028

Chambi-Peralta M, Vieira Coelho AC, de Souza Carvalho FM, Toffoli SM. 2018. Effects of exchanged cation, acid treatment and high shear mechanical treatment on the swelling and the particle size distribution of vermiculite. *Applied Clay Science,* **155**(4): 1-7. DOI: 10.1016/j.clay.2017.12.049

Chen C, Haibo L, Tianhu C, Dong C, Ray LF. 2015. An insight into the removal of Pb(II), Cu(II), Co(II), Cd(II), Zn(II), Ag(I), Hg(I), Cr(VI) by Na(I)-montmorillonite and Ca(II)-montmorillonite. *Applied Clay Science,* **118**: 239-247. DOI: 10.1016/j.clay.2015.09.004

Eren E, Afsin B. 2008. An investigation by raw and acid-activated bentonite: A combined potentiometric, thermodynamic, XRD, IR, DTA study. *J. Hazard Mater,* **151**(2-3): 682-691. DOI: 10.1016/j.jhazmat.2007.06.040

Eren E, Afsin B, Onal Y. 2009. Removal of lead ions by acid activated and manganese oxide-coated bentonite. *J. Haz. Mat,* **161**(2-3): 677-685. DOI: 10.1016/j.jhazmat.2008.04.020

Fonseca B, Maio H, Quintelas C, Teixeira A, Tavares T. 2009. Retention of Cr (VI) and Pb (II) on a loamy sand soil: Kinetics, equilibria and breakthrough. *Chem. Eng. J.,* **152**(1): 212-219. DOI: 10.1016/j.cej.2009.04.045

Ghorbel-Abid I, Trabelsi-Ayadi M. 2015. Competitive adsorption of heavy metals on local landfill clay. *Arabian Journal of Chemistry,* **8**(1): 25-31. DOI: 10.1016/j.arabjc.2011.02.030

Gouin CA, Aka N, Adiaffi B, Bamba BS, Soro N. 2016. Pollution saisonnière des sédiments de lagune par des métaux lourds (Cu, Pb et Zn) en zone tropicale humide : cas de la lagune Mondoukou (Sud-Est de la Côte d'Ivoire). *Int. J. Biol. Chem. Sci.,* **10**(2): 835-845. DOI: http://dx.doi.org/10.4314/ijbcs.v10i2.31

Kam S, Zerbo L, Bathiebo J, Soro J, Naba S, Wenmenga U, Traoré K, Gomina M, Blanchart P. 2009. Permeability to water of sintered clay ceramics. *Applied Clay Science,* **46**(4): 351-357. DOI: 10.1016/j.clay.2009.09.005

Karimi AS. 2011. Analysis of bentonite specific surface area by kinetic model during activation process in presence of sodium carbonate. *Microporous and Mesoporous Materials,* **141**(1-3): 81-87. DOI: 10.1016/j.micromeso.2010.10.031

Keita I, Sorgho B, Dembele C, Plea M, Zerbo L, Guel B, Ouedraogo R, Gomina M, Blanchart P. 2014. Ageing of clay and clay–tannin geomaterials for building. *Construction and Building Materials,* **61**(6): 114-119. DOI: 10.1016/j.conbuildmat.2014.03.005

Madejova J, Arvaiova B, Komadel P. 1999. FTIR spectroscopic characterization of thermally treated Cu2+, Cd2+ and Li+ montmorillonites. *Spectrochimica Acta Part A,* **55**(12): 2467-2476. DOI: 10.1016/S1386-1425(99)00039-6

Madejova J, Palkova H, Komabel P. 2006. Behaviour of Li+ and Cu2+ in heated montmorillonite: Evidence from far-, mid- and near-IR regions. *Vibrational Spectroscopy,* **40**(1): 80-88. DOI: 10.1016/j.vibspec.2005.07.004

Marsden MD, Philip A. 2003. Increased body lead burden-causes or consequences of chronic renal insufficiency. *The New England Journal of Medicine Editorials,* **348**: 345-347. DOI: 10.1056/NEJMe020164

Nila C, González I. 1996. Thermodynamics of Cu H2SO4 Cl− H2O and Cu NH4Cl H2O based on predominance-existence diagrams and Pourbaix-type diagrams. *Hydrometallurgy,* **42**(1): 63-82. DOI: 10.1016/0304-386X(95)00073-P

Nlend B, Celle-Jeanton H, Huneau F, Ketchemen-Tandia B, Etame J. 2018. The impact of urban development on aquifers in large coastal cities of West Africa: Present status and future challenges. *Land Use Policy,* **75**: 352-363. DOI: 10.1016/j.landusepol.2018.03.007

Okorie E, Olorunfemi CI. 2014. Monitoring the distribution of cadmium in sediment samples from Obajana stream in North central Nigeria. *Int. J. Biol. Chem. Sci.,* **8**(4): 1948-1954. DOI: http://dx.doi.org/10.4314/ijbcs.v8i4.54

Potgieter JH, Potgieter-Vermaak SS, Kalibantonga PD. 2006. Heavy metals removal from solution by palygorskite clay. *Minerals Engineering,* **19**(5): 463-470. DOI: 10.1016/j.mineng.2005.07.004

Rudnai T, Sándor J, Kádár M, Borsányi M, Rudnai P 2014. Arsenic in drinking water and congenital heart anomalies in Hungary. *International Journal of Hygiene and Environmental Health,* **217**(8): 813-818. DOI: 10.1016/j.ijheh.2014.05.002

Sajidu S, Persson I, Masamba WRL, Henry EMT, Kayambazinthu D. 2006. Removal of Cd2+, Cr3+, Cu2+, Hg2+, Pb2+ and Zn2+cations and AsO4- anions from aqueous solutions by mixed clay from Tundulu in Malawi and characterization of the clay. *Water SA,* **32**(4): 519-526. DOI: 10.1026/j.water.2006.04.519

Savic I, Gajic D, Stojiljkovic S, Savic I, di Gennaro S. 2014. Modelling and Optimization of Methylene Blue Adsorption from Aqueous Solution Using Bentonite Clay. *Computer Aided Chemical Engineering,* **33**: 1417-1422. DOI: 11.2016/j.Chem.Eng.2014.33.1417

Schütz T, Dolinská S, Hudec P, Mockovčiaková A, Znamenáčková I. 2016. Cadmium adsorption on manganese modified bentonite and bentonite–quartz sand blend. *International Journal of Mineral Processing,* **150**(5): 32-38. DOI: 10.1016/j.minpro.2016.03.003

Sorgho B, Ayouba Mahamane A, Guel B, Zerbo L, Gomina M, Blanchart P. 2016. Removal of Cd2+, Cu2+ and Pb2+ with a Burkina Faso clay. *Scientific Study & Research,* **17**(4): 365-379.

Srivastava P, Singh B, Angove M. 2005. Competitive adsorption behavior of heavy metals on kaolinite. *Journal of*

Colloid and Interface Science, **290**(1): 28-38. DOI:10.1016/j.jcis.2005.04.036

Tamungang NEB, Mvondo-Zé AD, Ghogomu JN, Mofor NA. 2016. Evaluation of phosphorus sorption characteristics of soils from the Bambouto sequence (West Cameroon). *Int. J. Biol. Chem. Sci.,* **10**(2): 860-874. DOI: http://dx.doi.org/10.4314/ijbcs.v10i2.33

Traoré K, Kabré TS, Blanchart P. 2000. Low temperature sintering of a pottery clay from Burkina Faso. *Applied Clay Science,* **17**(5–6): 279-292. DOI: S0169-1317 00 00020-X

UNIDO's Mercury Program. 2013. United Nations Industrial Development Organization (UNIDO), Vienna.

Yavuz O, Altunkaynak Y, Guzel F. 2003. Removal of copper, nickel, cobalt and manganese from aqueous solution by kaolinite. *Water Research,* **37**(4): 948-952. DOI: 10.1016/S0043-1354(02)00409-8

Zhang H, Tong Z, Wei T, Tang Y. 2012. Sorption characteristics of Pb(II) on alkaline Ca-bentonite. *Appl. Clay Science,* **65-66**(9): 21-23. DOI: 10.1016/j.clay.2012.06.010.